Author/s:
Goodwin, I;Larsen, KM;Sangchooli, A;Smith, RE;Banaschewski, T;Barker, GJ;Bokde, ALW;Brühl, R;Desrivières, S;Garavan, H;Gowland, P;Grigis, A;Heinz, A;Lemaitre, H;Martinot, JL;Martinot, MLP;Artiges, E;Nees, F;Orfanos, DP;Paus, T;Poustka, L;Smolka, MN;Vaidya, N;Walter, H;Whelan, R;Schumann, G;Hester, R;Garrido, MI

Title:
Psychotic-Like Experiences and White Matter Microstructure: A Fixel-Based Analysis Approach With Robust Replication Across Two Cohorts

Date:
2025-12-01

Citation:
Goodwin, I., Larsen, K. M., Sangchooli, A., Smith, R. E., Banaschewski, T., Barker, G. J., Bokde, A. L. W., Brühl, R., Desrivières, S., Garavan, H., Gowland, P., Grigis, A., Heinz, A., Lemaitre, H., Martinot, J. L., Martinot, M. L. P., Artiges, E., Nees, F., Orfanos, D. P. ,... Garrido, M. I. (2025). Psychotic-Like Experiences and White Matter Microstructure: A Fixel-Based Analysis Approach With Robust Replication Across Two Cohorts. Human Brain Mapping, 46 (17), pp.e70414-. https://doi.org/10.1002/hbm.70414.

Persistent Link:
https://hdl.handle.net/11343/368068

Human Brain Mapping

WILEY

RESEARCH ARTICLE OPEN ACCESS

Psychotic-Like Experiences and White Matter Microstructure: A Fixel-Based Analysis Approach With Robust Replication Across Two Cohorts

Isabella Goodwin[1] | Kit Melissa Larsen[2] | Arshiya Sangchooli[1,3] | Robert E. Smith[4,5] | Tobias Banaschewski[6] | Gareth J. Barker[7] | Arun L. W. Bokde[8] | Rüdiger Brühl[9] | Sylvane Desrivières[10] | Hugh Garavan[11] | Penny Gowland[12] | Antoine Grigis[13] | Andreas Heinz[14] | Herve Lemaitre[15] | Jean-Luc Martinot[16] | Marie-Laure Paillère Martinot[16,17] | Eric Artiges[16,18] | Frauke Nees[6,19] | Dimitri Papadopoulos Orfanos[20] | Tomáš Paus[21,22] | Luise Poustka[23] | Michael N. Smolka[24] | Nilakshi Vaidya[25] | Henrik Walter[14] | Robert Whelan[26] | Gunter Schumann[24,27] | IMAGEN Consortium | Robert Hester[1] | Marta I. Garrido[1,28]

[1]Melbourne School of Psychological Sciences, The University of Melbourne, Melbourne, Australia | [2]Danish Research Centre for Magnetic Resonance, Department of Radiology and Nuclear Medicine, Copenhagen University Hospital, Copenhagen, Denmark | [3]Turner Institute for Brain and Mental Health, Monash University, Heidelberg, Australia | [4]The Florey Institute of Neuroscienace and Mental Health, Heidelberg, Australia | [5]Florey Department of Neuroscience and Mental Health, The University of Melbourne, Melbourne, Australia | [6]Department of Child and Adolescent Psychiatry and Psychotherapy, Central Institute of Mental Health, Medical Faculty Mannheim, Heidelberg University, German Center for Mental Health (DZPG), Mannheim, Germany | [7]Department of Neuroimaging, Institute of Psychiatry, Psychology & Neuroscience, London, UK | [8]Discipline of Psychiatry, School of Medicine and Trinity College Institute of Neuroscience, Trinity College Dublin, Dublin, Ireland | [9]Physikalisch-Technische Bundesanstalt (PTB), Braunschweig, Germany | [10]Social, Genetic and Developmental Psychiatry Centre, Institute of Psychiatry, Psychology & Neuroscience, King's College London, London, UK | [11]Department of Psychiatry and Psychology, University of Vermont, Burlington, USA | [12]Sir Peter Mansfield Imaging Centre School of Physics and Astronomy, University of Nottingham, Nottingham, UK | [13]NeuroSpin, CEA, Gif-sur-Yvette, France | [14]Department of Psychiatry and Psychotherapy CCM, Charité—Universitätsmedizin Berlin, Corporate Member of Freie Universität Berlin, Humboldt-Universität Zu Berlin, and Berlin Institute of Health, Berlin, Germany | [15]Institut Des Maladies Neurodégénératives, UMR 5293, CNRS, CEA, Université de Bordeaux, Bordeaux, France | [16]Institut National de la Santé et de la Recherce Médicale, INSERM U A10 "Trajectoires développementales & Psychiatrie", University Paris-Saclay, Ecole Normale Supérieure Paris-Saclay, CNRS, Gif-sur-Yvette, France | [17]AP-HP. Sorbonne Université, Department of Child and Adolescent Psychiatry, Pitié-Salpêtrière Hospital, Paris, France | [18]Psychiatry Department, EPS Barthélémy Durand, Etampes, France | [19]Institute of Medical Psychology and Medical Sociology, University Medical Center Schleswig Holstein, Kiel University, Kiel, Germany | [20]Department of Psychology, School of Social Sciences, University of Mannheim, Mannheim, Germany | [21]Department of Psychiatry and Neuroscience, Faculty of Medicine and Centre Hospitalier Universitaire Sainte-Justine University of Montreal Quebec Canada, Montreal, Canada | [22]Department of Psychiatry, McGill University, Montreal, Canada | [23]Department of Child and Adolescent Psychiatry, Center for Psychosocial Medicine, University Hospital Heidelberg, Heidelberg, Germany | [24]Department of Psychiatry and Psychotherapy, Technische Universität Dresden, Dresden, Germany | [25]Centre for Population Neuroscience and Stratified Medicine (PONS), department of Psychiatry and Psychotherapy, Charité Universitätsmedizin Berlin, Berlin, Germany | [26]School of Psychology and Global Brain Health Institute, Trinity College Dublin, Dublin, Ireland | [27]Centre for Population Neuroscience and Precision Medicine (PONS), Institute for Science and Technology of Brain-Inspired Intelligence (ISTBI), Fudan University, Shanghai, China | [28]Graeme Clark Institute for Biomedical Engineering, The University of Melbourne, Melbourne, Australia

Correspondence: Isabella Goodwin (goodwin.isabella@gmail.com)

Received: 25 April 2025 | **Revised:** 9 November 2025 | **Accepted:** 11 November 2025

Keywords: diffusion-weighted imaging | fixel-based analysis | psychotic-like experiences | white matter

ABSTRACT

Structural deficits in white matter fibre have been linked to psychosis. However, it remains unclear whether these aberrations are present in individuals that experience non-clinical psychotic-like experiences, predating illness onset. While previous research demonstrates that alterations in white matter in schizotypy are consistent with those in clinical psychosis, these studies often

dichotomise healthy samples into high and low schizotypy, which may reduce statistical sensitivity. Previous research is also confounded by the investigation of diffusion MRI parameters that fail to account for complex crossing fibre populations. In this work, we treat psychotic-like experiences as a continuous variable, and applied Fixel-Based Analysis (FBA), a framework for investigating microstructural and morphological effects in brain white matter using diffusion-weighted imaging data. Across two independent cohorts of healthy participants with varied psychotic-like experiences including data from the IMAGEN consortium (Study 1 $n = 41$; Study 2 $n = 1098$), we hypothesized that greater psychotic-like experiences would be associated with FBA metrics sensitive to microstructural fibre density and/or cross-sectional morphological effects. Contrary to our hypothesis, we did not find significant correlations between psychotic-like experiences and FBA metrics across either dataset (FWE $p < 0.05$). Bayesian analysis of tract-aggregated data showed substantial evidence of no association (Bayes factor $< 1/3$) between psychotic-like experiences and fibre density, nor cross-sectional morphology, across several white matter tracts of interest, pre-defined from prior neuroimaging literature. These findings suggest that the relationship between non-clinical psychotic-like experiences and white matter microstructure may not be as robust as previously thought. This raises the possibility that white matter alterations across the psychosis spectrum echo clinical diagnostic thresholding, with observable effects in clinical but not sub-clinical presentations. Our findings show no association between whole-brain fibre-specific properties of white matter microstructure and sub-clinical psychotic-like experiences. Further, we show evidence for the lack of an association within tract-aggregated fibre-specific metrics. Future research should integrate longitudinal designs to explore whether fibre-specific white matter attributes provide clinically meaningful insight into the risk of psychosis onset.

1 | Introduction

Psychotic symptoms have been proposed to lie on a continuum distribution of severity, with varying degrees of psychotic-like experiences present in the general population (Guloksuz and van Os 2018). Psychotic-like experiences are thought to reflect a trait-like or phenotypic phenomenon, characterizable as an attenuation of positive psychotic symptom expression, namely hallucinations and delusions (van Os and Reininghaus 2016). Higher incidences of psychotic-like experiences are thought to reflect vulnerability or risk of transition to clinical psychosis such as first-episode psychosis or schizophrenia (Kaymaz et al. 2012). Investigating psychotic-like experiences could offer insight into commonalities across the extended continuum of psychosis, without the confounds of medication, hospitalization and comorbidity. The disconnection hypothesis of psychosis (Friston 1998; Friston and Frith 1995) suggests that clinical symptomatology such as hallucinations and delusions are attributable to widespread disturbances in connectivity between brain regions (Podwalski et al. 2021). Particularly, white matter microstructure, measured in vivo with diffusion-weighted imaging, consistently reveals decreased fractional anisotropy across prefrontal and temporal regions (for a review of evidence see Karlsgodt 2016; Kubicki et al. 2007).

Similar white matter abnormalities have been found across the extended continuum of psychosis. For example, robust differences in fractional anisotropy across the superior and inferior longitudinal fasciculi have been found in both people with schizophrenia and first-episode psychosis (Waszczuk et al. 2021). Additionally, the magnitude of white matter differences in fractional anisotropy in participants at ultra-high risk for psychosis was found to predict transition to schizophrenia at a later timepoint (Smigielski et al. 2022), and subtle white matter disturbances across frontal and temporal tracts have revealed relevancy for the risk of psychopathological onset (Boos et al. 2013). Despite heterogeneity in findings, some research investigating white matter deficits in schizotypy suggests consistency with clinical expression. For example, high schizotypy was found to be associated with lower fractional anisotropy in the inferior fronto-occipital fasciculus, as well as greater asymmetry (right > left) in the uncinate fasciculus (DeRosse et al. 2015). This is consistent with white matter deficits reported in a meta-analysis of first-episode psychosis patients (Yao et al. 2013) and has also been corroborated in individuals with heightened schizotypal traits (Lemaitre et al. 2018; Nelson et al. 2011; Oestreich et al. 2019b; Roddy et al. 2022). This supports the neurobiological continuum of aberrant white matter microstructure across clinical psychosis, individuals at risk for psychosis, and some evidence for continuity into non-clinical psychotic-like experiences.

Previous research often dichotomises neurotypical participants into 'high schizotypy' and 'low schizotypy', using arbitrary splitting techniques to impose artificial categorical boundaries on what should be considered a continuous scale (Linscott and van Os 2013). Further, of the few studies where continuous correlations between schizotypy and imaging markers have been interrogated, study inclusion has typically been limited to low-to-moderate schizotypy due to low sample sizes. Two recent studies addressed some of these limitations, investigating the association between white matter and psychotic-like experiences in a large, general population sample, using data from the UK BioBank (Bosma et al. 2021; Schoorl et al. 2021). In these studies, psychotic-like experiences in combination with distress were found to correlate with reduced global fractional anisotropy, suggesting that white matter microstructure seems to be altered in people who experience distressing psychotic-like experiences.

Another major limitation of previous white matter research in psychosis is the use of the diffusion tensor model, which is limited in its ability to correctly represent crossing fibre populations, leading to reduced biological specificity with consequential impact on interpretability (Tournier et al. 2011). This is problematic, given that as much as 90% of white matter voxels are thought to contain crossing fibres (Jeurissen et al. 2013). Voxel-aggregate measures such as Fractional Anisotropy (FA) may therefore be non-specific due to their sensitivity to both

microstructural properties and crossing fibre geometry. Higher-order diffusion models such as spherical deconvolution can attribute quantitative parameters to multiple individual fibre populations within a voxel ('fixels'). Further, a recent analytic framework tailored to operate on such data, Fixel-Based Analysis (FBA), allows statistical inference of effects in metrics reflecting microstructural and morphological properties of the white matter in a manner that is both sensitive and specific to this crossing fibre architecture.

While there has been a steady increase in studies employing FBA in recent years due to its ability to overcome the confounds of traditional voxel-based methods, it is yet to be used to investigate correlates of white matter microstructure across non-clinical psychotic-like experiences. In a recent study that used both voxel-based and fixel-based metrics in patients with schizophrenia compared to controls, fractional anisotropy as derived from the diffusion tensor model identified differences in crossing fibre regions, which were hypothesized as being indicative of group differences in crossing fibre organisation (Grazioplene et al. 2018). They also found that patients with schizophrenia exhibited lower fibre density (a metric derived from FBA) in the dorsal and posterior corpus callosum compared to healthy controls, reflecting microstructural group differences. Similarly, Stämpfli et al. (2019) found reduced fibre density in frontal fasciculi regions of patients with schizophrenia relative to controls, despite no corresponding difference in fractional anisotropy. These findings highlight the strength of FBA to move beyond classical voxel-based models, in favour of techniques that disambiguate different sources of white matter alterations associated with schizophrenia. Additionally, Kristensen et al. (2023) found that antipsychotic-naïve first-episode psychosis patients displayed reduced fibre density in the body of the corpus callosum and in the middle cerebellar peduncle compared to healthy controls, suggesting that white matter microstructure may be altered early in psychosis onset.

In this study, we used two cohorts of healthy participants to examine the relationship between psychotic-like experiences and white matter microstructure using FBA metrics sensitive to microstructural fibre density and cross-sectional morphological effects. In Study 1, participants ($n = 41$) were selectively sampled across an enriched distribution of psychotic-like experiences to allow for robust correlational analyses. In Study 2, we aimed to replicate these analyses in an independent sample ($n = 1098$) from the IMAGEN consortium (a multisite, international study of adolescent brain development and mental health; Mascarell Maričić et al. 2020), providing greater statistical power and a wider ecologically representative distribution of psychotic-like experiences.

2 | Methods

2.1 | Participants

2.1.1 | Study 1

Neuroimaging, demographic, and behavioural data were acquired from 52 healthy adults (aged 18–25), recruited through the Psychological Research Participation Scheme (SONA) at the University of Queensland. Prior screening excluded participants reporting a history of psychiatric or neurological disorders. During the screening process, participants completed the Community Assessment of Psychic Experiences (CAPE; Konings et al. 2006) which is used to assess psychotic-like experiences in healthy individuals. Participants were then selectively sampled from those that completed the screening process to yield a cohort for which the distribution of this score was approximately Gaussian. After screening, eligible participants then completed the 92-item Prodromal Questionnaire (PQ) which is also used to measure psychotic-like experiences in healthy individuals (Loewy et al. 2005). This self-report questionnaire has four subscales of symptom categories: positive, negative, disorganised and general. As we were interested in drawing parallels between the primary symptoms in schizophrenia (i.e., hallucinations and delusions, also referred to as positive symptoms) and those in non-clinical individuals, this study exclusively used the positive symptom subscale (PQ-positive) as our primary measure of psychotic-like experiences. PQ-positive was selected for primary analysis due to issues with missing data from CAPE-positive in the final sample. Possible scores for the PQ-positive subscale range from 45 to 225. Participants provided written informed consent and received monetary reimbursement for their time. This research was approved by the University of Queensland Human Research Ethics. After quality control (see section 'Data Exclusions'), 41 participants were included in the final sample.

2.1.2 | Study 2

Neuroimaging, demographic and behavioural data were obtained from the IMAGEN consortium (Mascarell Maričić et al. 2020; Schumann et al. 2010; https://imagen-europe.com), which comprises 2315 adolescents included at age 14 and followed up until age 22 with three waves after initial baseline testing across eight European sites with local ethics research committees approving the study at each site. At the time the consortium database was accessed, data were unavailable from the London site; thus only data from the other seven sites were analysed. For the primary analysis, we identified 1411 participants who had both behavioural and neuroimaging data available at age 18.

Several behavioural and cognitive measures were collected as part of the IMAGEN study. Participants completed the CAPE questionnaire (Konings et al. 2006). The CAPE is a 42-item self-report questionnaire that has been developed and validated to measure the dimensions of psychosis in the general population. The CAPE has a three-factor structure with dimensions of positive, negative, and depressive symptoms. Participants are asked to rate each item on a Likert scale ranging 1–4 for both the frequency of experiences ('Never', 'Sometimes', 'Often', or 'Nearly always') and distress associated with these experiences ('Not distressing', 'A bit distressing', 'Quite distressing', or 'Very distressing'). The frequency scores were used for the main analysis while the distress scores were used for exploratory analyses. The positive symptom frequency subscale (CAPE-positive) was used as our primary measure of psychotic-like experiences. Possible scores for the CAPE-positive frequency subscale range from 20 to 80. After quality control (see section 'Data Exclusions'), 1098 participants were included in the final sample.

2.2 | Neuroimaging Acquisition

2.2.1 | Study 1

Data were acquired on a Siemens 3 T Prisma scanner with a 64-channel head coil. For the structural scan, T1-weighted magnetization-prepared rapid gradient-echo (MPRAGE) images were acquired with the following parameters: repetition time TR = 4 s, echo time TE = 2.91 ms, flip angle = 6.7° and an isotropic resolution of 1.0 mm with matrix size = [176240256]. Diffusion-weighted images (DWI) were acquired using an echo-planar imaging sequence with the following parameters: 30 diffusion-weighted volumes with b-value = 1200s/mm^2, 60 volumes with b-value = 2500 s/mm^2, and 6 volumes without diffusion weighting; 68 oblique-axial slices (angled parallel to the anterior commissure/posterior commissure line); repetition time TR = 4.1 s, echo time TE = 75 ms; 122 × 122 matrix; field of view 244 × 244 mm; voxel size = 2.0 × 2.0 × 2.0 mm.

2.2.2 | Study 2

Data were acquired across a range of 3 T scanners: Siemens scanners were used across 5 scanning sites (Berlin, Dresden, Hamburg, Mannheim, Paris), with the remaining two sites using Philips scanners (Dublin, Nottingham). Structural T1-weighted MPRAGE images were based on the ADNI protocol (https://adni.loni.usc.edu/data-samples/adni-data/neuroimaging/mri/mri-scanner-protocols/) and had an isotropic resolution of 1.1 mm. DWI data were acquired using echo-planar imaging sequences with the following parameters: 32 diffusion-weighted volumes with b-value = 1300s/mm^2 and 4 volumes without diffusion weighting; 60 oblique-axial slices; repetition time TR = 15 s, echo time TE = 104 ms; 128 × 128 matrix; field of view 307 × 307 mm; voxel size = 2.4 × 2.4 × 2.4 mm.

2.3 | Anatomical Image Preprocessing

In order to calculate estimates of intracranial volumes (eICV) to be used as a covariate in the main analysis (Smith et al. 2019), the default FreeSurfer pipeline (Version 7.3.2; Buckner et al. 2004; Fischl 2012; Smith et al. 2019) was run on T1-weighted images to reconstruct brain surfaces in Study 1; for Study 2 the pre-computed estimates provided by the IMAGEN dataset were used.

2.4 | Diffusion Image Preprocessing

Data were preprocessed according to the recommended pipeline of FBA (Raffelt, Tournier, et al. 2017) using MRtrix version 3.0.4 (Tournier et al. 2019; http://www.mrtrix.org). The workflow was performed independently for Study 1 and Study 2, with minor differences in the analysis pipelines detailed throughout this section (see Figure 1 for a summary). Across both cohorts, DWI underwent denoising (Veraart et al. 2016) and Gibbs ringing removal (Kellner et al. 2016) before correcting for motion and eddy-current distortions (Andersson and Sotiropoulos 2016). Characteristic tissue response functions were estimated individually from each participant's preprocessed DWI (Dhollander et al. 2016, 2019).

2.5 | Fixel Based Analysis (FBA)

In Study 1, individual response functions were averaged across all participants to generate group average response functions (Raffelt, Tournier, Rose, et al. 2012). Multi-Shell, Multi-Tissue Constrained Spherical Deconvolution (MSMT-CSD; Jeurissen et al. 2014) was then used to decompose the DWI signal into each voxel into a white matter Fibre Orientation Distribution (FOD) in addition to contributions from macroscopic grey matter and cerebrospinal fluid (CSF). Following this, intensity normalisation based on the multi-tissue decomposition was performed (Dhollander, Tabbara, et al. 2021; Raffelt, Dhollander, et al. 2017). An unbiased study-specific population template was generated using white matter FODs of all 41 participants (Raffelt et al. 2011).

In Study 2, group-level global intensity normalization was run based on the median $b = 0$ intensity in white matter (Raffelt, Tournier, Rose, et al. 2012), before individual response function estimation. Site-specific group average response functions were computed to ensure valid inter-participant comparisons while controlling for scanner differences across sites (Meisler and Gabrieli 2022). Since DWI data were all obtained with a single non-zero b-value, Single-Shell 3-Tissue Constrained Spherical Deconvolution (SS3T-CSD; Dhollander and Connelly 2016) was utilized to obtain FODs of white matter, gray matter, and CSF for each participant (Dhollander, Clemente, et al. 2021). An unbiased study-specific population template was generated using white matter FODs from a subset of 42 participants for computational tractability (Raffelt et al. 2011). To maximize template quality, included in this subset were, from each of the seven scanning sites, the six participants with the highest quality control prediction score (Meisler and Gabrieli 2022; Richie-Halford et al. 2022).

The following steps were completed independently across both studies. Participant FOD images were registered to the population template for their study using non-linear registration, with reorientation using apodised point spread functions (Raffelt, Tournier, Crozier, et al. 2012). The same transformation was used to warp brain masks to population template space. Participants with poor alignment of warped brain masks based on manual visual inspection were excluded from subsequent analyses (see section on 'Data Exclusions' for details). A whole-brain template-space analysis mask was calculated as the intersection of all participants' warped masks. Within each study's voxel-wise template mask, a template fixel dataset was obtained through segmentation of the study FOD template (Smith et al. 2013). Participant fixels were segmented from their warped FODs (Smith et al. 2013), and reoriented according to the non-linear transformation (Raffelt, Tournier, et al. 2017). For each template fixel, correspondence with the nearest subject fixel was established provided their orientations differed by no more than 45° (Raffelt, Tournier, et al. 2017).

The fixel-wise metrics of fibre density (FD), fibre-bundle cross section (FC), and a combined metric of fibre density and cross section (FDC) were computed for inferential analysis (Raffelt, Tournier, et al. 2017). FD, a measure of white matter microstructure which is ideally proportional to intra-axonal volume, was calculated as the integrals of the FOD lobes in the warped participant FOD image from which the participant fixels were derived (Raffelt, Tournier, et al. 2017; Smith et al. 2013). FC, which is

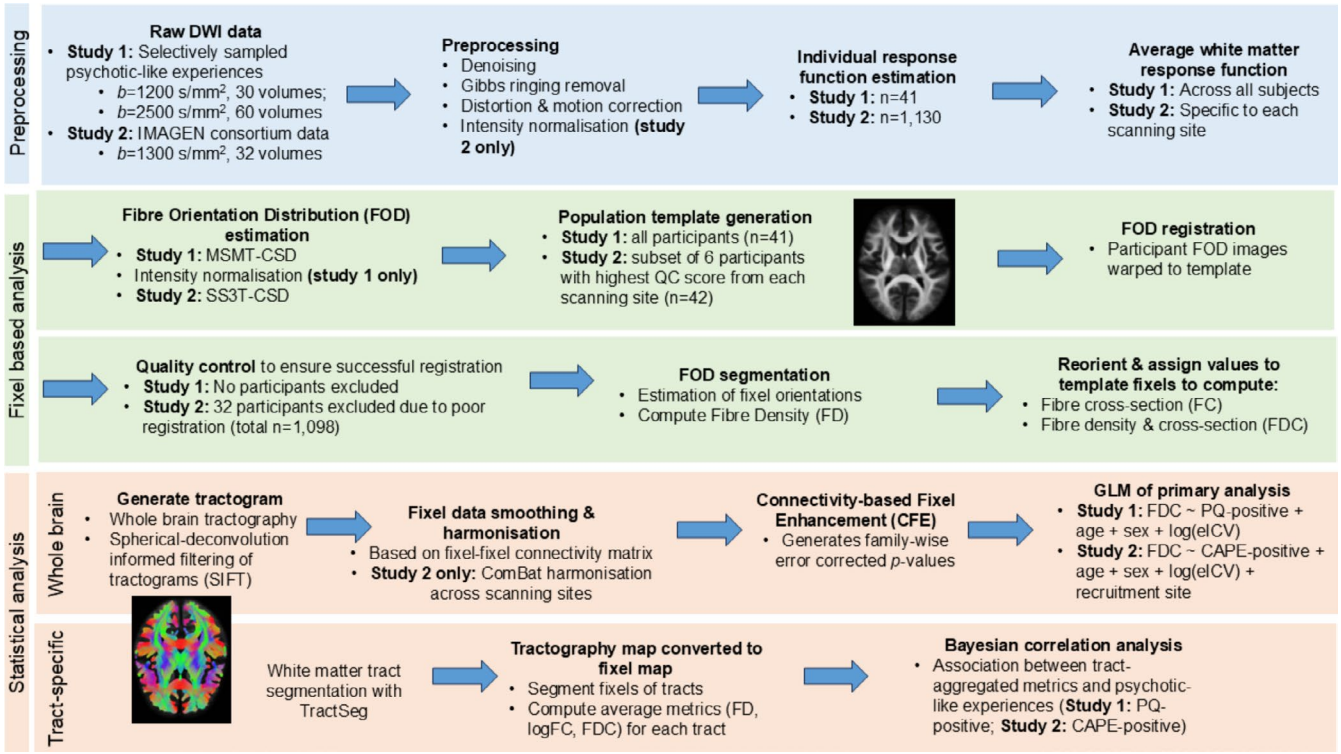

FIGURE 1 | Schematic summarising key steps of Fixel-Based Analysis pipeline, highlighting differences between Study 1 and Study 2. CAPE = community assessment of psychic experiences; CFE = connectivity-based fixel enhancement; DWI = diffusion weighted imaging; eICV = estimated intracranial volume; FC = fibre cross-section; FD = fibre density; FDC = fibre density and cross-section; FOD = fibre orientation distribution; GLM = general linear model; PQ = prodromal questionnaire; QC = quality check; SIFT = spherical-deconvolution informed filtering of tractograms. Examples from Study 1 of group-level FOD template (row 2) and whole-brain tractogram (row 4) are shown. Flowchart design based on Fan et al. (2024) and Genc et al. (2018).

proportional to the macroscopic cross-section of the white matter fibre bundle, was calculated as a measure of the local geometric distortions required to warp a participant's FOD to template space (Raffelt, Tournier, et al. 2017). FDC was calculated as the product of these two. Where FC was assessed in isolation, values were log-transformed to ensure zero mean and normality.

For each study, a whole-brain tractogram with 20 million streamlines was generated from the FOD template with uniformly distributed seeding using the iFOD2 algorithm (Tournier et al. 2010). SIFT (Smith et al. 2013) was applied to filter the tractogram to 2 million streamlines to reduce reconstruction biases (Maier-Hein et al. 2017). Filtered tractograms were used to create a fixel-fixel connectivity matrix for each study. This connectivity data was used to inform spatial smoothing of FD, logFC and FDC maps (Raffelt et al. 2015). To correct for inter-site variability (study 2 only), ComBat harmonisation (Fortin et al. 2017) for fixel data (FixelComBat; Mito et al. 2023, 2024) was applied after data smoothing prior to statistical analysis.

2.6 | Tract Segmentation

Across both studies, we also employed a tract-of-interest approach using TractSeg (Wasserthal et al. 2018; https://github.com/MIC-DKFZ/TractSeg), an automated method that provides segmentation of 72 major white matter tracts. As an input to this method, we extracted up to three spherical harmonic peaks in each voxel of the population template FOD image (Jeurissen et al. 2013). Tracts of interest for this study were selected based on previous findings of white matter aberrations in the continuum of psychosis (DeRosse et al. 2015; Grazioplene et al. 2018; Kristensen et al. 2023; Stämpfli et al. 2019): cingulum bundles (CG), corpus callosum (CC), inferior fronto-occipital fasciculi (IFOF), inferior longitudinal fasciculi (ILF), superior longitudinal fasciculi (SLF) and uncinate fasciculi (UF). To obtain a single SLF tract per hemisphere, we merged SLF I, SLF II and SLF III subcomponents from the tractography outputs from TractSeg, resulting in one combined tractogram for the left SLF and right SLF. A similar process was used to combine subsections of the CC, to obtain a single CC tract file. For each bundle of interest, we generated the default 2000 streamlines per tract, computed the number of streamlines assigned to each template fixel, and binarized these data to produce a fixel mask per tract. The tractography of tracts of interest is visually presented in Figure 2.

2.7 | Statistics

2.7.1 | Whole-Brain Analysis

Whole-brain fixel-based statistical inference was performed using Connectivity-based Fixel Enhancement (CFE; Raffelt et al. 2015), with familywise error correction for multiple comparisons using non-parametric permutation testing at a significance threshold $\alpha = 0.05$. For our primary analyses, we limited our analyses to the FDC metric only (Smith et al. 2021), regressing

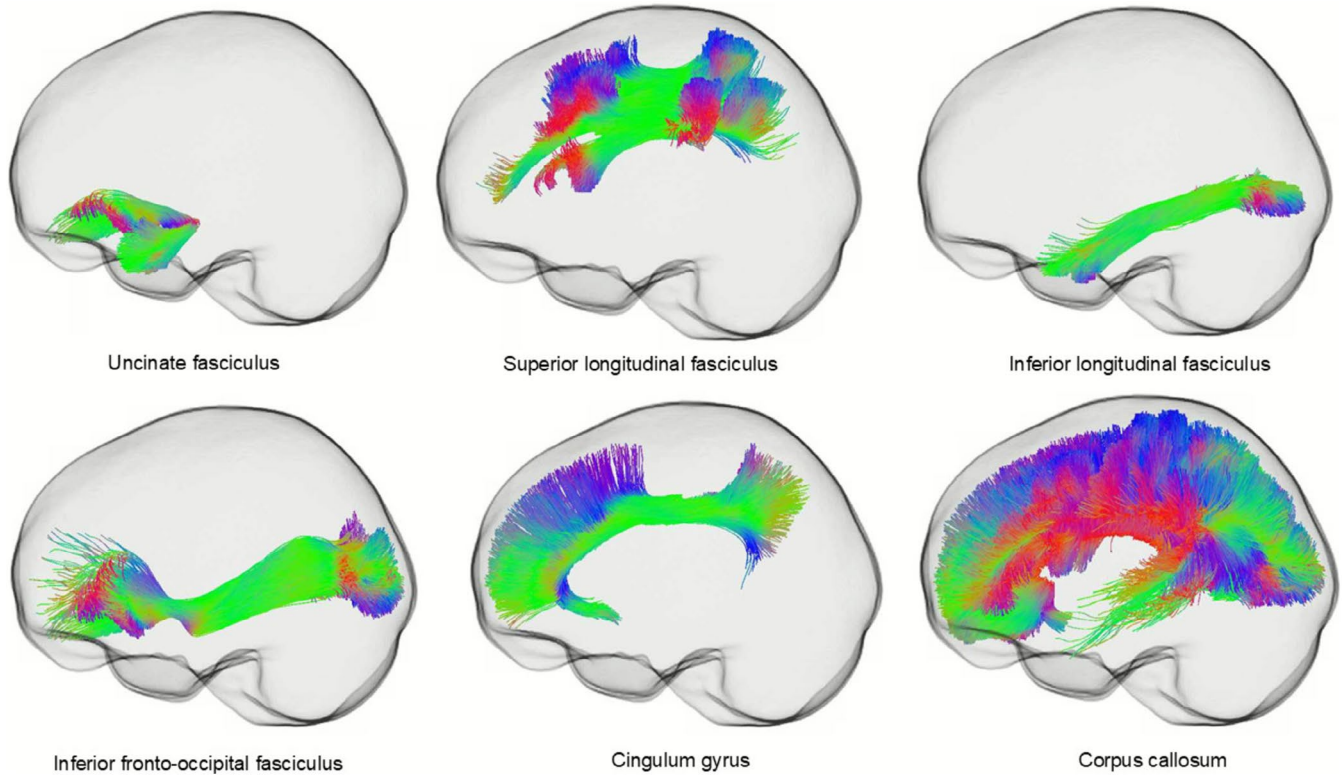

FIGURE 2 | White matter tractography pathways extracted in Study 1, showing left hemispheric view of fibre pathways presented on a sagittal slice of a 3D glass brain reconstruction with MRtrix. The same tracts of interest were generated across both studies (with only Study 1 shown for simplicity). All tracts except for the corpus callosum were considered bilaterally, meaning that 11 tracts were analysed in total per study.

against PQ-positive scores in Study 1 and CAPE-positive scores in Study 2 (two *t*-tests; positive and negative direction of association). Potential confounds we included as covariates in our statistical model were age (Han et al. 2023; Kelley et al. 2021), sex (Kirkovski et al. 2020; Lyon et al. 2019), and log-transformed eICV (Smith et al. 2019). In Study 2 only, we also included the recruitment site as a covariate to account for residual variability not corrected with ComBat harmonisation. All variables were standardized (*z*-score transformation) before statistical analyses were run. As a secondary data investigation, we also ran analogous models for FD and logFC to explore the relative contribution of microstructure and morphometry, with log(eICV) omitted as a covariate for the FD model (Smith et al. 2019).

2.7.2 | Tract-Specific Analysis

The frequentist analysis approach (i.e., null hypothesis significant testing) has been criticised for its inability to determine evidence in support of the null hypothesis where non-significant *p*-values are obtained (Wagenmakers et al. 2018). Alternatively, Bayesian analysis can quantify evidence for both the alternative and the null hypothesis, providing improved reporting specificity for non-significant *p*-values. A Bayesian framework was utilised here for tract-aggregated data, to determine whether there was substantial evidence in support of, or against, an association between psychotic-like experiences and white matter measures in the 11 pre-defined tracts of interest. This tract-based Bayesian analysis followed a similar approach to Fan et al. (2024). Tract-aggregated values of FBA metrics (FDC, FD and logFC) were computed within the fixel masks of each tract of interest. Bayesian correlation analysis between tract-averaged FDC, FD and logFC values and psychotic-like experiences was performed for both studies. The evidence for an association between tract-aggregated data and psychotic-like experiences was represented by the Bayes factor (BF_{10}): $BF_{10} > 3$ was considered substantial evidence for the alternative hypothesis, while $BF_{10} < 1/3$ was considered substantial evidence for the null hypothesis, based on recommended strength of evidence classification schemes (Jarosz and Wiley 2014; Jeffreys and Jeffreys 1998; Raftery 1995). Bayesian analysis was conducted with the *BayesFactor* and *BayestestR* packages (Makowski et al. 2019) in R (version 4.2.2), specifically implementing the correlationBF() function with a uniform, non-informative prior over the correlation coefficient, ranging from −1 to 1.

2.8 | Exploratory Analysis

Given that psychotic-like experiences when weighted by distress have been found to be indicative of psychosis risk (Jaya et al. 2021), we also explored the role of distress in Study 2, using data on participants' attribution of distress to their psychotic-like experiences (see section 'Participants: Study 2'). For this, we computed scores for severity-weighted psychotic-like experiences by multiplying the frequency score with the associated distress score for each item (Jaya et al. 2021). We ran a regression of FDC against CAPE severity-weighted positive scores (with analogous models for FD and logFC as secondary analyses), including the same covariates as detailed in the previous section. Tract-based Bayesian correlation analysis between tract-averaged metrics (FDC, FD and logFC) and CAPE

severity-weighted positive scores was also performed. As distress scores were only available from data collected in Study 2, analogous models were not run for Study 1.

2.9 | Data Exclusions

2.9.1 | Study 1

Of the 52 participants recruited, we excluded participants who had missing PQ scores ($n=2$), missing DWI data ($n=3$), or failed *FreeSurfer* reconstruction ($n=6$). Based on these criteria, a total of 41 participants were included in analyses. Participants' transformed brain masks were overlaid on top of the FOD template as a quality control check to ensure registration was successful. In this cohort, no participants were excluded due to poor registration after visual inspection.

2.9.2 | Study 2

Of the 2315 participants who completed follow-up two of the IMAGEN study, we excluded participants who had missing CAPE scores ($n=91$), missing DWI data ($n=904$), failed *FreeSurfer* reconstruction ($n=8$), preprocessing errors (e.g., issues with diffusion gradient encoding; $n=182$), or poor registration to the population FOD template by visual inspection (as described in the previous section; $n=32$), leading to a total of 1098 included in the analysis.

3 | Results

3.1 | Participant Characteristics

Demographic characteristics of participants across both studies are shown in Table 1, with the final sample consisting of 41 participants in Study 1 (26 female, 15 male), and 1098 participants in Study 2 (572 female, 526 male). For Study 2, demographic characteristics separated by scanning site are provided in Supporting Information. The distribution of psychotic-like experiences across both studies (i.e., PQ-positive for Study 1 and CAPE-positive for Study 2) is shown in Figure 3.

3.2 | Fixel-Based Analysis

3.2.1 | Whole-Brain Approach

For Study 1, whole-brain CFE analysis revealed no significant positive or negative correlation between PQ-positive scores and FDC, adjusted for age, sex and log(eICV). This means that there were no fixels anywhere in the brain where FDC values were significantly associated with PQ-positive scores across participants at significance threshold $\alpha=0.05$. For an example of the template data, Figure 4 shows the template fixels coloured by beta-coefficient values of PQ-positive scores when associated with FDC. Similarly for Study 2, whole-brain CFE analysis revealed no significant positive or negative correlation between CAPE-positive scores and FDC, adjusting for age, sex and log(eICV) and scanning site.

Secondary analyses to investigate the magnitude of effects in FD and logFC metrics in Study 1 revealed no significant correlation between PQ-positive scores and FD (adjusting for age and sex) nor between scores and logFC (adjusting for age, sex and log(eICV)). Similarly, secondary analyses for Study 2 revealed no significant correlation between CAPE-positive scores and FD (adjusting for age and sex) nor between scores and logFC (adjusting for age, sex and log(eICV)).

3.2.2 | Tract-Specific Approach

Tract-based analyses revealed no significant positive or negative correlation between psychotic-like experiences (PQ-scores in Study 1; CAPE-positive scores in Study 2) and FD (adjusting for age and sex in both studies, as well as scanning site in Study 2) across the 11 tracts of interest depicted in Figure 2. In Study 1, Bayesian analysis of tract-aggregated white matter metrics

TABLE 1 | Participant characteristics across studies.

	Study 1 ($n=41$)		Study 2 ($n=1098$)	
	Mean (sd)	**Median [range]**	**Mean (sd)**	**Median [range]**
Age, years	21.15 (1.93)	21.0 [18.0–25.0]	18.53 (0.74)	18.0 [18.0–23.0]
ICV (cm^3)	1362.72 (145.29)	1342.57 [1174.62–1825.05]	1542.32 (155.83)	1533.20 [1083.67–2118.01]
PQ-positive	62.02 (13.65)	61.0 [44.0–101.0]	—	—
PQ-negative	31.10 (11.25)	30.0 [17.0–78.0]	—	—
PQ-disorganised	23.8 (7.19)	22.0 [13.0–41.0]	—	—
PQ-general	26.32 (7.67)	25.0 [16.0–54.0]	—	—
CAPE-total	—	—	61.55 (11.42)	60.0 [42.0–123.0]
CAPE-positive	—	—	25.89 (4.63)	25.0 [20.0–57.0]
CAPE-negative	—	—	22.19 (5.45)	21.5 [14.0–45.0]
CAPE-depressive	—	—	13.47 (3.44)	13.0 [8.0–30.0]

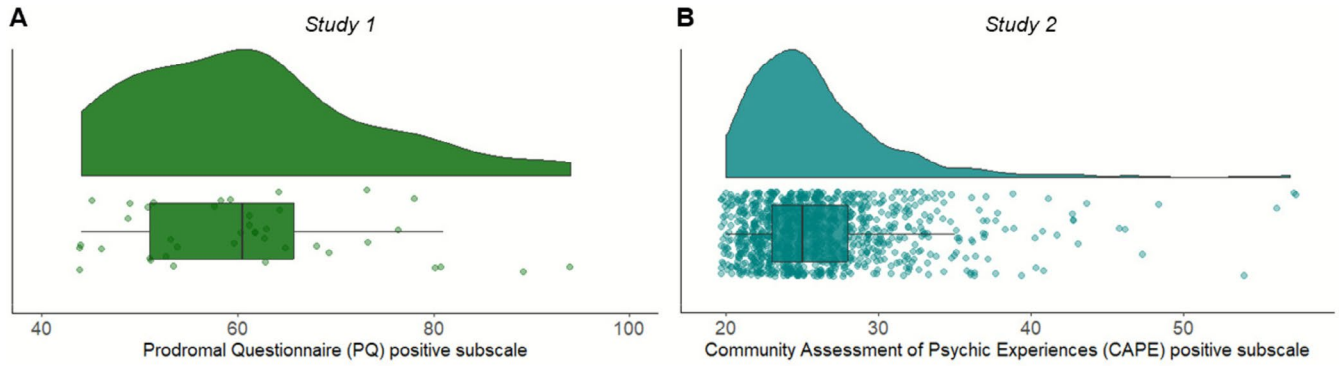

FIGURE 3 | Distribution of psychotic-like experiences across (A) Study 1 (PQ-positive scores) and (B) Study 2 (CAPE-positive scores). Each dot represents the score of an individual participant on the corresponding questionnaire. Boxplots demonstrate the median and interquartile range of psychotic-like experience scores across each study.

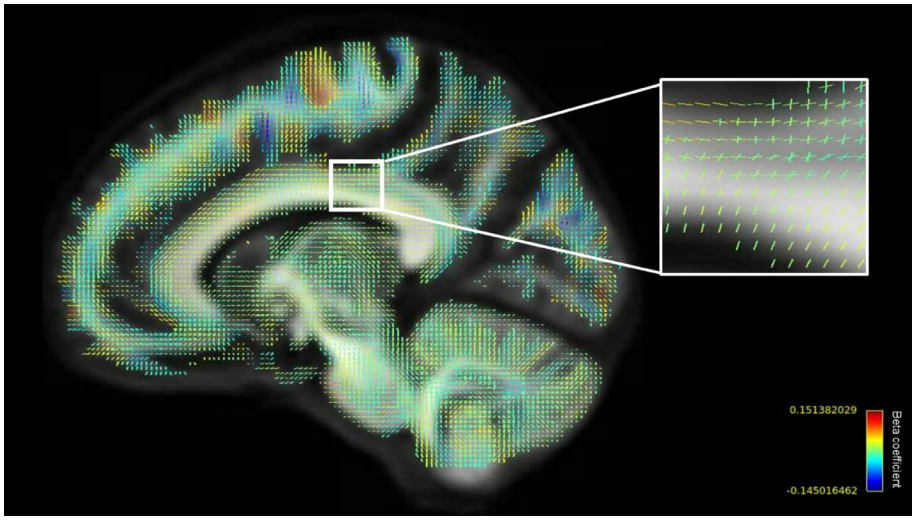

FIGURE 4 | Whole-brain fixel-based analysis showing template fixels coloured by the beta coefficient of psychotic-like experiences associated with FDC in Study 1, including regions of crossing fibres. Template fixels coloured by the beta coefficient corresponding to psychotic-like experiences (PQ-positive) associated with FDC values in Study 1, with no fixels reaching statistical significance. Shown for a single sagittal slice with the zoomed inset showing specific fixels in crossing-fibre regions, with fixels coloured by beta coefficient values.

showed weak evidence in favour of the null hypothesis (i.e., no association between FDC, FD, nor logFC and psychotic-like experiences) for all white matter tracts of interest, with the exception of tract-aggregated FD and psychotic-like experiences in left SLF showing weak evidence in favour of the alternative hypothesis (see Table 2). In Study 2, Bayesian analysis of tract-aggregated data showed substantial evidence to support the null hypothesis in almost all white matter tracts of interest, with the exception of tract-aggregated FD and psychotic-like experiences in the corpus callosum where evidence in favour of the null hypothesis was only weak (see Table 3). See Table S2 for the number of fixels in each tract.

3.3 | Exploratory Analyses: CAPE Severity-Weighted Positive Scores (Study 2 Only)

3.3.1 | Whole-Brain Approach

Whole-brain FBA results revealed no significant positive or negative correlation between CAPE severity-weighted positive scores (i.e., frequency weighted by distress scores) and FDC (as the primary analysis), FD, or logFC (as secondary analyses), adjusted for age, sex, log(eICV) where applicable, and scanning site.

3.3.2 | Tract-Specific Approach

Bayesian analysis of tract-aggregated white matter metrics showed substantial evidence to support the null hypothesis (i.e., no association between FDC, FD nor logFC and severity-weighted psychotic-like experiences) in all 11 white matter tracts of interest (see Table 4).

4 | Discussion

This study presents the first application of fixel-based analysis to investigate fibre-specific white matter microstructure of participants with varying psychotic-like experiences. Contrary to our hypothesis, we did not find any associations between white matter and non-clinical psychotic-like experiences, across two independent cohorts with different diffusion MRI acquisitions and quantitative measures of psychotic-like experiences.

TABLE 2 | Bayesian correlation between tract-average FBA metrics and psychotic-like experiences (PQ-positive) in Study 1 in 11 white matter tracts of interest.

		FD			logFC			FDC		
WM tract		**β**	**95% CI**	**BF_{10}**	**β**	**95% CI**	**BF_{10}**	**β**	**95% CI**	**BF_{10}**
CC		−0.16	−0.43 to 0.14	0.63	−0.04	−0.33 to 0.26	0.36	−0.08	−0.35 to 0.22	0.40
CG	Lt	−0.03	−0.31 to 0.26	0.35	−0.04	−0.31 to 0.24	0.36	−0.04	−0.33 to 0.26	0.36
	Rt	0.02	−0.25 to 0.31	0.36	−0.06	−0.34 to 0.23	0.38	−0.05	−0.32 to 0.25	0.37
IFO	Lt	−0.21	−0.46 to 0.08	0.98	−0.06	−0.33 to 0.23	0.38	−0.13	−0.4 to 0.18	0.51
	Rt	−0.18	−0.44 to 0.1	0.76	−0.09	−0.36 to 0.2	0.42	−0.12	−0.39 to 0.16	0.51
ILF	Lt	−0.15	−0.41 to 0.15	0.56	−0.07	−0.33 to 0.21	0.39	−0.11	−0.37 to 0.19	0.45
	Rt	−0.19	−0.45 to 0.1	0.82	−0.08	−0.35 to 0.22	0.40	−0.13	−0.41 to 0.16	0.52
SLF	Lt	−0.24	−0.49 to 0.05	1.29	−0.14	−0.41 to 0.15	0.56	−0.19	−0.45 to 0.1	0.82
	Rt	−0.16	−0.43 to 0.15	0.63	−0.09	−0.37 to 0.19	0.41	−0.12	−0.4 to 0.17	0.48
UF	Lt	−0.13	−0.39 to 0.16	0.51	−0.07	−0.34 to 0.23	0.38	−0.11	−0.38 to 0.18	0.46
	Rt	−0.20	−0.46 to 0.09	0.91	−0.02	−0.31 to 0.27	0.35	−0.13	−0.41 to 0.15	0.53

Abbreviations: 95% CI = credible intervals for the model coefficient; BF_{10} = Bayes factor; CC = corpus callosum; CG = cingulum bundle; IFOF = inferior fronto-occipital fasciculus; ILF = inferior longitudinal fasciculus; Lt = left tract; Rt = right tract; SLF = superior longitudinal fasciculus; UF = uncinate fasciculus; β = standardised model coefficient (median of posterior distribution).

TABLE 3 | Bayesian correlation between tract-average FBA metrics and psychotic-like experiences (CAPE-positive) in Study 2 in 11 white matter tracts of interest.

		FD			logFC			FDC		
WM tract		**β**	**95% CI**	**BF_{10}**	**β**	**95% CI**	**BF_{10}**	**β**	**95% CI**	**BF_{10}**
CC		−0.06	−0.12 to 0	0.44	−0.02	−0.08 to 0.04	0.09*	−0.04	−0.1 to 0.01	0.19*
CG	Lt	−0.03	−0.09 to 0.03	0.12*	−0.02	−0.07 to 0.04	0.08*	−0.03	−0.09 to 0.03	0.11*
	Rt	−0.02	−0.08 to 0.03	0.10*	0	−0.06 to 0.05	0.07*	−0.02	−0.08 to 0.04	0.08*
IFO	Lt	−0.03	−0.09 to 0.03	0.12*	0.01	−0.05 to 0.06	0.07*	−0.02	−0.07 to 0.04	0.08*
	Rt	−0.02	−0.08 to 0.04	0.10*	0.02	−0.04 to 0.07	0.08*	0	−0.06 to 0.06	0.07*
ILF	Lt	−0.03	−0.09 to 0.03	0.12*	0.01	−0.05 to 0.07	0.08*	−0.01	−0.07 to 0.05	0.07*
	Rt	−0.01	−0.08 to 0.04	0.08*	0	−0.06 to 0.06	0.07*	0	−0.06 to 0.05	0.07*
SLF	Lt	−0.04	−0.09 to 0.02	0.14*	−0.02	−0.07 to 0.04	0.09*	−0.03	−0.09 to 0.03	0.13*
	Rt	−0.05	−0.11 to 0.01	0.27*	−0.01	−0.07 to 0.05	0.08*	−0.03	−0.09 to 0.02	0.14*
UF	Lt	−0.01	−0.07 to 0.05	0.08*	0.01	−0.05 to 0.06	0.07*	−0.01	−0.07 to 0.05	0.07*
	Rt	0.01	−0.05 to 0.07	0.07*	0	−0.06 to 0.06	0.07*	0	−0.06 to 0.06	0.07*

Abbreviations: 95% CI = credible intervals for the model coefficient; BF_{10} = Bayes factor; CC = corpus callosum; CG = cingulum bundle; IFOF = inferior fronto-occipital fasciculus; ILF = inferior longitudinal fasciculus; Lt = left tract; Rt = right tract; SLF = superior longitudinal fasciculus; UF = uncinate fasciculus; β = standardised model coefficient (median of posterior distribution).
*Substantial evidence for the null hypothesis ($BF_{10} < 1/3$).

Additionally, Bayesian analysis of data aggregated within tracts of interest based on prior studies revealed widespread evidence of no association between white matter quantitative measures and psychotic-like experiences; only weakly in the smaller Study 1 (CC, right SLF, and bilateral CG, ILF, IFOF and UF), but with substantial evidence of such in the much larger Study 2 (bilateral CG, ILF, SLF, IFOF and UF).

Previous literature has demonstrated robust changes in fixel-specific metrics reflecting white matter pathology in the clinical continuum of psychosis, specifically across people with schizophrenia (Grazioplene et al. 2018; Stämpfli et al. 2019) and first-episode psychosis (Kristensen et al. 2023). While past research using voxel-based diffusion-tensor metrics suggested analogous correlates of white matter aberrancies are present

TABLE 4 | Bayesian correlation between tract-average FBA metrics and severity-weighted psychotic-like experiences (CAPE-positive frequency × distress) in Study 2 in 11 white matter tracts of interest.

		FD			logFC			FDC		
WM tract		β	**95% CI**	BF_{10}	β	**95% CI**	BF_{10}	β	**95% CI**	BF_{10}
CC		−0.04	−0.1 to 0.02	0.18*	−0.03	−0.09 to 0.03	0.11*	−0.04	−0.1 to 0.02	0.19*
CG	Lt	−0.04	−0.1 to 0.02	0.20*	−0.03	−0.09 to 0.03	0.12*	−0.05	−0.1 to 0.01	0.21*
	Rt	−0.02	−0.07 to 0.04	0.08*	−0.02	−0.08 to 0.04	0.08*	−0.02	−0.08 to 0.03	0.10*
IFO	Lt	−0.04	−0.1 to 0.01	0.18*	−0.01	−0.07 to 0.05	0.08*	−0.03	−0.09 to 0.03	0.13*
	Rt	−0.02	−0.08 to 0.04	0.09*	0	−0.06 to 0.06	0.07*	−0.01	−0.07 to 0.05	0.07*
ILF	Lt	−0.03	−0.09 to 0.03	0.13*	−0.01	−0.06 to 0.05	0.07*	−0.02	−0.08 to 0.03	0.10*
	Rt	−0.02	−0.08 to 0.04	0.09*	−0.02	−0.07 to 0.04	0.08*	−0.02	−0.08 to 0.04	0.09*
SLF	Lt	−0.04	−0.1 to 0.02	0.19*	−0.03	−0.09 to 0.03	0.12*	−0.05	−0.11 to 0.02	0.22*
	Rt	−0.05	−0.11 to 0	0.37	−0.02	−0.08 to 0.03	0.10*	−0.04	−0.1 to 0.02	0.20*
UF	Lt	−0.03	−0.09 to 0.03	0.12*	−0.03	−0.09 to 0.03	0.11*	−0.04	−0.1 to 0.02	0.18*
	Rt	−0.01	−0.07 to 0.05	0.07*	−0.02	−0.08 to 0.04	0.08*	−0.02	−0.07 to 0.04	0.08*

Abbreviations: 95% CI = credible intervals for the model coefficient; BF_{10} = Bayes factor; CC = corpus callosum; CG = cingulum bundle; IFOF = inferior fronto-occipital fasciculus; ILF = inferior longitudinal fasciculus; Lt = left tract; RT = right tract; SLF = superior longitudinal fasciculus; UF = uncinate fasciculus; β = standardised model coefficient (median of posterior distribution).
*Substantial evidence for the null hypothesis ($BF_{10} < 1/3$).

in non-clinical psychotic-like experiences (DeRosse et al. 2015; Nelson et al. 2011; Oestreich et al. 2019a), we found no corresponding effects in this FBA study. Recent comparison between voxel-based and fixel-based metrics in patients with schizophrenia compared to controls demonstrated inconsistencies in group differences between methodological approaches (Grazioplene et al. 2018). As FBA provides a more biologically plausible model, particularly in regions with crossing fibres, voxel-based metrics of white matter may be largely capturing information about group differences in crossing fibre organisation, rather than microstructural differences attributable to specific pathways. Thus, our findings reflect a lack of association between white matter microstructure and psychotic-like experiences, through the utilisation of a more biologically plausible model than what was employed in previous research. To further confirm this finding, future research requires direct comparison between voxel-wise and fixel-wise correlates of psychotic-like experiences, particularly in regions of crossing fibres, to provide further support for the more recent fibre-specific approaches to measuring white matter microstructure.

There are, however, other voxel-based studies concordant with our negative findings. One recent study showed that attenuated subclinical psychotic symptoms in non-help-seeking individuals were not associated with white matter structural alterations (Michielse et al. 2020). Similarly, Koivukangas et al. (2015) reported an absence of microstructural white matter differences in young adults at familial risk for psychosis compared to controls. Together, these findings question the proposed continuity between clinical and non-clinical psychotic-like experiences in aberrations of white matter microstructure. White matter deficits may only emerge at illness onset or in prominent prodromal stages of psychosis such as first-episode psychosis (Kristensen et al. 2023), rather than pre-dating illness onset. While, collectively, this may suggest that white matter alterations echo clinical diagnostic thresholding with observable effects present in clinical, but not sub-clinical presentations, longitudinal research is required to further explore the nature of (dis)continuity associated with white matter microstructure, before and after illness onset.

Additionally, some research has suggested that the association between psychotic-like experiences and white matter microstructure is mediated by other factors that confer psychosis risk. For example, associations between psychotic-like experiences and aberrant white matter microstructure have been found to be more marked in participants that designate those experiences as distressing (Bosma et al. 2021; Schoorl et al. 2021). While this motivated corresponding exploratory analyses in the current study, these revealed no significant association—indeed substantial evidence of no association—between white matter microstructure and psychotic-like experiences when weighted by distress. Future research is therefore needed to examine both the complex non-linear nature of white matter changes associated with the full spectrum of psychoses, and whether distress interacts with such. Similarly, some research suggests that white matter deficits coincide with the introduction of antipsychotic medication in clinical populations (Szeszko et al. 2014), which could provide an alternative explanation of our null findings in never-medicated, healthy individuals with non-clinical psychotic-like experiences. However, a recent review of diffusion tensor imaging studies investigating the effect of white matter microstructure in first-episode drug-naïve patients demonstrated that white matter deficits precede antipsychotic medication (Sagarwala and Nasrallah 2021). While the findings are mixed, some studies even found an increase in fractional anisotropy after antipsychotic treatment. Given the sparsity of literature, future research is required to clearly delineate

the effects of antipsychotics on white matter microstructure in psychosis.

A strength of the current study was that it used a robust FBA framework to characterise white matter microstructure, overcoming the limitations inherent in traditional voxel-based methods with enhanced biological specificity. The findings from data analysed with FBA techniques suggest that the relationship between white matter microstructure and psychotic-like experiences may not be as robust as previously thought. Additionally, our findings were independently replicated across two cohorts of participants, which overcomes limitations of previous literature such as low sample sizes and lack of replication. An important utility of large, open-source datasets like the IMAGEN consortium is that they provide the enhanced statistical power required to detect small effect sizes, while also reducing the risk of false positive findings (Button et al. 2013). This is exemplified by stronger evidence of no association between tract-aggregated FBA metrics and psychotic-like experiences in Study 2 as compared to Study 1, which may have been underpowered to find strong evidence of no association given the smaller sample size of Study 1. Similarly, replication across independent cohorts improves the confidence in findings compared to analysis of a single dataset alone. Nevertheless, we should be cautious when interpreting findings from Bayesian approaches with uninformative priors applied to multiple tracts, particularly in Study 1 given the lower sample size. Similarly, evidence for the lack of association is derived from large, tract-aggregated fibre-specific metrics, which should be interpreted with caution. Given that large tracts were included in analyses (e.g., the entire corpus callosum rather than specific segments), smaller, highly specific regions may still be affected, as Bayesian analysis was not performed at each individual fixel.

While replicated across two independent cohorts, the generalisability of our findings is limited by certain attributes of those cohorts. The findings from this study may not apply to more age-diverse samples, given their limited age ranges (Study 1: 18–25; Study 2: 18–23). Additionally, the *b*-value (which impacts the estimation of DWI measures such as fibre density) of DWI obtained in Study 2 was relatively low compared to values typically employed by FBA (Dhollander, Clemente, et al. 2021; Genc et al. 2020), which may impact the sensitivity and specificity of fibre density estimates. Although this limitation was mitigated by the higher *b*-values present in Study 1, future research should consider adopting higher *b*-values to improve fibre density estimates (Raffelt, Tournier, Rose, et al. 2012).

To empirically verify whether aberrancies in white matter truly predate illness onset or are otherwise predictive of such transition, future research should employ longitudinal assessment of white matter microstructure and psychotic-like experiences in healthy populations that later transition to clinical psychosis. Doing so will improve our understanding of neurobiological markers of psychosis risk. The cross-sectional nature of this study means that it is unclear whether higher scores for psychotic-like experiences are predictive of later transition to clinical psychosis. However, given the longitudinal nature of the IMAGEN consortium dataset, the stability of psychotic-like experience scores relative to metrics of white matter fibre density and cross-sectional morphology could be assessed, despite a low transition rate to clinical psychosis (only 16 adolescents received a diagnosis of psychosis at follow-up, aged 23 years; Maitra et al. 2023).

5 | Conclusion

This study used both whole-brain and tract-specific fixel-based analysis to characterise fibre-specific white matter microstructure and morphology in two cohorts of participants with a spectrum of non-clinical psychotic-like experiences. Our findings show no association between whole-brain fibre-specific properties of white matter microstructure and non-clinical psychotic-like experiences. Further, we show evidence for the lack of an association within tract-aggregated fibre-specific metrics. While these findings extend our understanding of white matter microstructure across the extended psychosis continuum, future research is required to determine whether characterising fibre-specific white matter attributes provides clinically meaningful insight into the risk of psychosis onset.

Acknowledgements

This work received support from the following sources: the European Union-funded FP6 Integrated Project IMAGEN (Reinforcement-related behaviour in normal brain function and psychopathology) (LSHM-CT- 2007-037286), the Horizon 2020 funded ERC Advanced Grant 'STRATIFY' (Brain network based stratification of reinforcement-related disorders) (695313), Horizon Europe 'environMENTAL', grant no: 101057429, UK Research and Innovation (UKRI) Horizon Europe funding guarantee (10041392 and 10038599), Human Brain Project (HBP SGA 2, 785907, and HBP SGA 3, 945539), the Chinese government via the Ministry of Science and Technology (MOST). The German Center for Mental Health (DZPG), the Bundesministerium für Bildung und Forschung (BMBF grants 01GS08152; 01EV0711; Forschungsnetz AERIAL 01EE1406A, 01EE1406B; Forschungsnetz IMAC-Mind 01GL1745B), the Deutsche Forschungsgemeinschaft (DFG project numbers 458317126 [COPE], 186318919 [FOR 1617], 178833530 [SFB 940], 386691645 [NE 1383/14-1], 402170461 [TRR 265], 454245598 [IRTG 2773]), the Medical Research Foundation and Medical Research Council (grants MR/R00465X/1 and MR/S020306/1), the National Institutes of Health (NIH) funded ENIGMA-grants 5U54EB020403-05, 1R56AG058854-01 and U54 EB020403 as well as NIH R01DA049238, the National Institutes of Health, Science Foundation Ireland (16/ERCD/3797). NSFC grant 82150710554. Further support was provided by grants from:—the ANR (ANR-12-SAMA-0004, AAPG2019—GeBra), the Eranet Neuron (AF12-NEUR0008-01—WM2NA; and ANR-18-NEUR00002-01—ADORe), the Fondation de France (00081242), the Fondation pour la Recherche Médicale (DPA20140629802), the Mission Interministérielle de Lutte-contre-les-Drogues-et-les-Conduites-Addictives (MILDECA), the Assistance-Publique-Hôpitaux-de-Paris and INSERM (interface grant), Paris Sud University IDEX 2012, the Fondation de l'Avenir (grant AP-RM-17-013), the Fédération pour la Recherche sur le Cerveau. This work was supported by the Australian Research Council (ARC) Centre of Excellence for Integrative Brain Function (ARC CE140100007) to M.I.G. K.M.L. received funding from the Lundbeck Foundation (R322-2019-2311). RS is supported by fellowship funding from the National Imaging Facility (NIF), an Australian Government National Collaborative Research Infrastructure Strategy (NCRIS) capability.

Funding

This work was supported by the Australian Research Council (ARC) Centre of Excellence for Integrative Brain Function (ARC CE140100007) to M.I.G. K.M.L. received funding from the Lundbeck Foundation

(R322-2019-2311). RS is supported by fellowship funding from the National Imaging Facility (NIF), an Australian Government National Collaborative Research Infrastructure Strategy (NCRIS) capability.

Conflicts of Interest

Tobias Banaschewski served in an advisory or consultancy role for AGB Pharma, eye level, Infectopharm, Medice, Neurim Pharmaceuticals, Oberberg GmbH and Takeda. He received conference support or a speaker's fee from Janssen-Cilag, Medice and Takeda. He received royalties from Hogrefe, Kohlhammer, CIP Medien, Oxford University Press; the present work is unrelated to these relationships. Gareth J. Barker has received honoraria from General Electric Healthcare for teaching on scanner programming courses. Luise Poustka served in an advisory or consultancy role for Roche and Viforpharm and received a speaker's fee from Shire. She received royalties from Hogrefe, Kohlhammer and Schattauer. Associate editor is a co-author—Tomáš Paus is a handling editor of Human Brain Mapping and a co-author of this article. To minimise bias, they were excluded from all editorial decision-making related to the acceptance of this article for publication. The present work is unrelated to the above grants and relationships. The other authors report no biomedical financial interests or potential conflicts of interest.

Data Availability Statement

The data that support the findings of this study are available from the corresponding author upon reasonable request.

References

Andersson, J. L. R., and S. N. Sotiropoulos. 2016. "An Integrated Approach to Correction for Off-Resonance Effects and Subject Movement in Diffusion MR Imaging." *NeuroImage* 125: 1063–1078. https://doi.org/10.1016/j.neuroimage.2015.10.019.

Boos, H. B. M., R. C. W. Mandl, N. E. M. van Haren, et al. 2013. "Tract-Based Diffusion Tensor Imaging in Patients With Schizophrenia and Their Non-Psychotic Siblings." *European Neuropsychopharmacology* 23, no. 4: 295–304. https://doi.org/10.1016/j.euroneuro.2012.05.015.

Bosma, M. J., S. R. Cox, T. Ziermans, et al. 2021. "White Matter, Cognition and Psychotic-Like Experiences in UK Biobank." *Psychological Medicine* 53: 1–2379. https://doi.org/10.1017/S0033291721004244.

Buckner, R. L., D. Head, J. Parker, et al. 2004. "A Unified Approach for Morphometric and Functional Data Analysis in Young, Old, and Demented Adults Using Automated Atlas-Based Head Size Normalization: Reliability and Validation Against Manual Measurement of Total Intracranial Volume." *NeuroImage* 23, no. 2: 724–738. https://doi.org/10.1016/j.neuroimage.2004.06.018.

Button, K. S., J. P. A. Ioannidis, C. Mokrysz, et al. 2013. "Power Failure: Why Small Sample Size Undermines the Reliability of Neuroscience." *Nature Reviews Neuroscience* 14, no. 5: 365–376. https://doi.org/10.1038/nrn3475.

DeRosse, P., G. C. Nitzburg, T. Ikuta, B. D. Peters, A. K. Malhotra, and P. R. Szeszko. 2015. "Evidence From Structural and Diffusion Tensor Imaging for Frontotemporal Deficits in Psychometric Schizotypy." *Schizophrenia Bulletin* 41, no. 1: 104–114. https://doi.org/10.1093/schbul/sbu150.

Dhollander, T., A. Clemente, M. Singh, et al. 2021. "Fixel-Based Analysis of Diffusion MRI: Methods, Applications, Challenges and Opportunities." *NeuroImage* 241: 118417. https://doi.org/10.1016/j.neuroimage.2021.118417.

Dhollander, T., and A. Connelly. 2016. "A Novel Iterative Approach to Reap the Benefits of Multi-Tissue CSD From Just Single-Shell (+b=0) Diffusion MRI Data." https://www.researchgate.net/publication/301766619_A_novel_iterative_approach_to_reap_the_benefits_of_multi-tissue_CSD_from_just_single-shell_b0_diffusion_MRI_data.

Dhollander, T., R. Mito, D. Raffelt, and A. Connelly. 2019. "Improved White Matter Response Function Estimation for 3-Tissue Constrained Spherical Deconvolution." https://www.researchgate.net/publication/331165168_Improved_white_matter_response_function_estimation_for_3-tissue_constrained_spherical_deconvolution.

Dhollander, T., D. Raffelt, and A. Connelly. 2016. "Unsupervised 3-Tissue Response Function Estimation From Single-Shell or Multi-Shell Diffusion MR Data Without a Co-Registered T1 Image. 5." https://www.researchgate.net/profile/Thijs-Dhollander/publication/307863133_Unsupervised_3-tissue_response_function_estimation_from_single-shell_or_multi-shell_diffusion_MR_data_without_a_co-registered_T1_image/links/57cfb5c708ae83b374623e5a/Unsupervised-3-tissue-response-function-estimation-from-single-shell-or-multi-shell-diffusion-MR-data-without-a-co-registered-T1-image.pdf.

Dhollander, T., R. Tabbara, J. Rosnarho-Tornstrand, J.-D. Tournier, D. Raffelt, and A. Connelly. 2021. "Multi-Tissue Log-Domain Intensity and Inhomogeneity Normalisation for Quantitative Apparent Fibre Density." https://archive.ismrm.org/2021/2472.html.

Fan, F., R. Beare, S. Genc, et al. 2024. "White Matter Fiber Morphology in Persisting Postconcussive Symptoms and Posttraumatic Headache After Pediatric Concussion: A Fixel-Based Analysis." *Journal of Neurosurgery. Pediatrics* 34, no. 4: 373–383. https://doi.org/10.3171/2024.6.PEDS2499.

Fischl, B. 2012. "FreeSurfer." *NeuroImage* 62, no. 2: 774–781. https://doi.org/10.1016/j.neuroimage.2012.01.021.

Fortin, J.-P., D. Parker, B. Tunç, et al. 2017. "Harmonization of Multi-Site Diffusion Tensor Imaging Data." *NeuroImage* 161: 149–170. https://doi.org/10.1016/j.neuroimage.2017.08.047.

Friston, K. 1998. "The Disconnection Hypothesis." *Schizophrenia Research* 30, no. 2: 115–125. https://doi.org/10.1016/S0920-9964(97)00140-0.

Friston, K., and C. D. Frith. 1995. "Schizophrenia: A Disconnection Syndrome?" *Clinical Neuroscience* 3, no. 2: 89–97.

Genc, S., R. E. Smith, C. B. Malpas, et al. 2018. "Development of White Matter Fibre Density and Morphology Over Childhood: A Longitudinal Fixel-Based Analysis." *NeuroImage* 183: 666–676. https://doi.org/10.1016/j.neuroimage.2018.08.043.

Genc, S., C. Tax, E. Raven, M. Chamberland, G. Parker, and D. Jones. 2020. "Impact of b-Value on Estimates of Apparent Fibre Density." *Human Brain Mapping* 41, no. 10: 2583–2595. https://doi.org/10.1002/hbm.24964.

Grazioplene, R. G., C. E. Bearden, K. L. Subotnik, et al. 2018. "Connectivity-Enhanced Diffusion Analysis Reveals White Matter Density Disruptions in First Episode and Chronic Schizophrenia." *NeuroImage. Clinical* 18: 608–616. https://doi.org/10.1016/j.nicl.2018.02.015.

Guloksuz, S., and J. van Os. 2018. "The Slow Death of the Concept of Schizophrenia and the Painful Birth of the Psychosis Spectrum." *Psychological Medicine* 48, no. 2: 229–244. https://doi.org/10.1017/S0033291717001775.

Han, A., T. Dhollander, Y. L. Sun, J. A. Chad, and J. J. Chen. 2023. "Fiber-Specific Age-Related Differences in the White Matter of Healthy Adults Uncovered by Fixel-Based Analysis." *Neurobiology of Aging* 130: 22–29. https://doi.org/10.1016/j.neurobiolaging.2023.06.007.

Jarosz, A. F., and J. Wiley. 2014. "What Are the Odds? A Practical Guide to Computing and Reporting Bayes Factors." *Journal of Problem Solving* 7, no. 1: 2. https://doi.org/10.7771/1932-6246.1167.

Jaya, E. S., T. van Amelsvoort, A. A. Bartels-Velthuis, et al. 2021. "The Community Assessment of Psychic Experiences: Optimal Cut-Off Scores for Detecting Individuals With a Psychotic Disorder." *International Journal of Methods in Psychiatric Research* 30, no. 4: e1893. https://doi.org/10.1002/mpr.1893.

Jeffreys, S. H., and S. H. Jeffreys. 1998. *The Theory of Probability*. 3rd ed. Oxford University Press.

Jeurissen, B., A. Leemans, J.-D. Tournier, D. K. Jones, and J. Sijbers. 2013. "Investigating the Prevalence of Complex Fiber Configurations in White Matter Tissue With Diffusion Magnetic Resonance Imaging." *Human Brain Mapping* 34, no. 11: 2747–2766. https://doi.org/10.1002/hbm.22099.

Jeurissen, B., J.-D. Tournier, T. Dhollander, A. Connelly, and J. Sijbers. 2014. "Multi-Tissue Constrained Spherical Deconvolution for Improved Analysis of Multi-Shell Diffusion MRI Data." *NeuroImage* 103: 411–426. https://doi.org/10.1016/j.neuroimage.2014.07.061.

Karlsgodt, K. H. 2016. "Diffusion Imaging of White Matter in Schizophrenia: Progress and Future Directions." *Biological Psychiatry: Cognitive Neuroscience and Neuroimaging* 1, no. 3: 209–217. https://doi.org/10.1016/j.bpsc.2015.12.001.

Kaymaz, N., M. Drukker, R. Lieb, et al. 2012. "Do Subthreshold Psychotic Experiences Predict Clinical Outcomes in Unselected Non-Help-Seeking Population-Based Samples? A Systematic Review and Meta-Analysis, Enriched With New Results." *Psychological Medicine* 42, no. 11: 2239–2253. https://doi.org/10.1017/S0033291711002911.

Kelley, S., J. Plass, A. R. Bender, and T. A. Polk. 2021. "Age-Related Differences in White Matter: Understanding Tensor-Based Results Using Fixel-Based Analysis." *Cerebral Cortex (New York, N.Y.: 1991)* 31, no. 8: 3881–3898. https://doi.org/10.1093/cercor/bhab056.

Kellner, E., B. Dhital, V. G. Kiselev, and M. Reisert. 2016. "Gibbs-Ringing Artifact Removal Based on Local Subvoxel-Shifts." *Magnetic Resonance in Medicine* 76, no. 5: 1574–1581. https://doi.org/10.1002/mrm.26054.

Kirkovski, M., I. Fuelscher, C. Hyde, et al. 2020. "Fixel Based Analysis Reveals Atypical White Matter Micro- and Macrostructure in Adults With Autism Spectrum Disorder: An Investigation of the Role of Biological Sex." *Frontiers in Integrative Neuroscience* 14: 40. https://doi.org/10.3389/fnint.2020.00040.

Koivukangas, J., L. Björnholm, O. Tervonen, et al. 2015. "White Matter Structure in Young Adults With Familial Risk for Psychosis – The Oulu Brain and Mind Study." *Psychiatry Research: Neuroimaging* 233, no. 3: 388–393. https://doi.org/10.1016/j.pscychresns.2015.06.015.

Konings, M., M. Bak, M. Hanssen, J. Van Os, and L. Krabbendam. 2006. "Validity and Reliability of the CAPE: A Self-Report Instrument for the Measurement of Psychotic Experiences in the General Population." *Acta Psychiatrica Scandinavica* 114, no. 1: 55–61. https://doi.org/10.1111/j.1600-0447.2005.00741.x.

Kristensen, T. D., J. M. Raghava, M. W. Skjerbæk, et al. 2023. "Fibre Density and Fibre-Bundle Cross-Section of the Corticospinal Tract Are Distinctly Linked to Psychosis-Specific Symptoms in Antipsychotic-naïve Patients With First-Episode Schizophrenia." *European Archives of Psychiatry and Clinical Neuroscience* 273, no. 8: 1797–1812. https://doi.org/10.1007/s00406-023-01598-7.

Kubicki, M., R. McCarley, C.-F. Westin, et al. 2007. "A Review of Diffusion Tensor Imaging Studies in Schizophrenia." *Journal of Psychiatric Research* 41, no. 1–2: 15–30. https://doi.org/10.1016/j.jpsychires.2005.05.005.

Lemaitre, A.-L., G. Lafargue, H. Duffau, and G. Herbet. 2018. "Damage to the Left Uncinate Fasciculus Is Associated With Heightened Schizotypal Traits: A Multimodal Lesion-Mapping Study." *Schizophrenia Research* 197: 240–248. https://doi.org/10.1016/j.schres.2018.02.027.

Linscott, R. J., and J. van Os. 2013. "An Updated and Conservative Systematic Review and Meta-Analysis of Epidemiological Evidence on Psychotic Experiences in Children and Adults: On the Pathway From Proneness to Persistence to Dimensional Expression Across Mental Disorders." *Psychological Medicine* 43, no. 6: 1133–1149. https://doi.org/10.1017/S0033291712001626.

Loewy, R. L., C. E. Bearden, J. K. Johnson, A. Raine, and T. D. Cannon. 2005. "The Prodromal Questionnaire (PQ): Preliminary Validation of a Self-Report Screening Measure for Prodromal and Psychotic Syndromes." *Schizophrenia Research* 79, no. 1: 117–125.

Lyon, M., T. Welton, A. Varda, et al. 2019. "Gender-Specific Structural Abnormalities in Major Depressive Disorder Revealed by Fixel-Based Analysis." *NeuroImage: Clinical* 21: 101668. https://doi.org/10.1016/j.nicl.2019.101668.

Maier-Hein, K. H., P. F. Neher, J.-C. Houde, et al. 2017. "The Challenge of Mapping the Human Connectome Based on Diffusion Tractography." *Nature Communications* 8, no. 1: 1349. https://doi.org/10.1038/s41467-017-01285-x.

Maitra, R., C. M. Horne, O. O'Daly, et al. 2023. "Psychotic Like Experiences in Healthy Adolescents Are Underpinned by Lower Fronto-Temporal Cortical Gyrification: A Study From the IMAGEN Consortium." *Schizophrenia Bulletin* 49, no. 2: 309–318. https://doi.org/10.1093/schbul/sbac132.

Makowski, D., M. S. Ben-Shachar, and D. Lüdecke. 2019. "bayestestR: Describing Effects and Their Uncertainty, Existence and Significance Within the Bayesian Framework." *Journal of Open Source Software* 4, no. 40: 1541. https://doi.org/10.21105/joss.01541.

Mascarell Maričić, L., H. Walter, A. Rosenthal, et al. 2020. "The IMAGEN Study: A Decade of Imaging Genetics in Adolescents." *Molecular Psychiatry* 25, no. 11: 2648–2671. https://doi.org/10.1038/s41380-020-0822-5.

Meisler, S. L., and J. D. Gabrieli. 2022. "Fiber-Specific Structural Properties Relate to Reading Skills in Children and Adolescents." *eLife* 11: e82088. https://doi.org/10.7554/eLife.82088.

Michielse, S., I. Lange, J. Bakker, et al. 2020. "White Matter Microstructure and Network-Connectivity in Emerging Adults With Subclinical Psychotic Experiences." *Brain Imaging and Behavior* 14, no. 5: 1876–1888. https://doi.org/10.1007/s11682-019-00129-0.

Mito, R., M. Pedersen, H. Pardoe, et al. 2024. "Exploring Individual Fixel-Based White Matter Abnormalities in Epilepsy." *Brain Communications* 6, no. 1: fcad352. https://doi.org/10.1093/braincomms/fcad352.

Mito, R., R. Smith, J.-D. Tournier, D. N. Vaughan, M. Pedersen, and G. D. Jackson. 2023. "ComBat Scanner Harmonisation for Fixel-Based Analysis." https://www.scilit.com/publications/ad71ed3fbe093d7a20a5701f34fb33be.

Nelson, M. T., M. L. Seal, L. J. Phillips, A. H. Merritt, R. Wilson, and C. Pantelis. 2011. "An Investigation of the Relationship Between Cortical Connectivity and Schizotypy in the General Population." *Journal of Nervous and Mental Disease* 199, no. 5: 348–353. https://doi.org/10.1097/NMD.0b013e318217514b.

Oestreich, L. K. L., R. Randeniya, and M. I. Garrido. 2019a. "Auditory Prediction Errors and Auditory White Matter Microstructure Associated With Psychotic-Like Experiences in Healthy Individuals." *Brain Structure and Function* 224, no. 9: 3277–3289. https://doi.org/10.1007/s00429-019-01972-z.

Oestreich, L. K. L., R. Randeniya, and M. I. Garrido. 2019b. "White Matter Connectivity Reductions in the Pre-Clinical Continuum of Psychosis: A Connectome Study." *Human Brain Mapping* 40, no. 2: 529–537. https://doi.org/10.1002/hbm.24392.

Podwalski, P., K. Szczygieł, E. Tyburski, L. Sagan, B. Misiak, and J. Samochowiec. 2021. "Magnetic Resonance Diffusion Tensor Imaging in Psychiatry: A Narrative Review of Its Potential Role in Diagnosis." *Pharmacological Reports* 73, no. 1: 43–56. https://doi.org/10.1007/s43440-020-00177-0.

Raffelt, D., T. Dhollander, J.-D. Tournier, et al. 2017. "Bias Field Correction and Intensity Normalisation for Quantitative Analysis of Apparent Fibre Density." *International Society for Magnetic Resonance in Medicine*. https://www.researchgate.net/profile/Thijs-Dhollander/publication/315836355_Bias_Field_Correction_and_Intensity_Normalisation_for_Quantitative_Analysis_of_Apparent_Fibre_Density/links/58fd20fcaca2723d79dbca87/Bias-Field-Correction-and-Inten

sity-Normalisation-for-Quantitative-Analysis-of-Apparent-Fibre-Density.pdf?__cf_chl_tk=dwi9WOWTd3rpQkz_G3HjW7jBba2Qr1EFDyOpS0ugarU-1738204183-1.0.1.1-ASPJBEMfQVvaa1HzckjAvFLBhVhD5qQt_LcC2aqL99o.

Raffelt, D., R. E. Smith, G. R. Ridgway, et al. 2015. "Connectivity-Based Fixel Enhancement: Whole-Brain Statistical Analysis of Diffusion MRI Measures in the Presence of Crossing Fibres." *NeuroImage* 117: 40–55. https://doi.org/10.1016/j.neuroimage.2015.05.039.

Raffelt, D., J.-D. Tournier, S. Crozier, A. Connelly, and O. Salvado. 2012. "Reorientation of Fiber Orientation Distributions Using Apodized Point Spread Functions." *Magnetic Resonance in Medicine* 67, no. 3: 844–855. https://doi.org/10.1002/mrm.23058.

Raffelt, D., J.-D. Tournier, J. Fripp, S. Crozier, A. Connelly, and O. Salvado. 2011. "Symmetric Diffeomorphic Registration of Fibre Orientation Distributions." *NeuroImage* 56, no. 3: 1171–1180. https://doi.org/10.1016/j.neuroimage.2011.02.014.

Raffelt, D., J.-D. Tournier, S. Rose, et al. 2012. "Apparent Fibre Density: A Novel Measure for the Analysis of Diffusion-Weighted Magnetic Resonance Images." *NeuroImage* 59, no. 4: 3976–3994. https://doi.org/10.1016/j.neuroimage.2011.10.045.

Raffelt, D., J.-D. Tournier, R. E. Smith, et al. 2017. "Investigating White Matter Fibre Density and Morphology Using Fixel-Based Analysis." *NeuroImage* 144: 58–73. https://doi.org/10.1016/j.neuroimage.2016.09.029.

Raftery, A. E. 1995. "Bayesian Model Selection in Social Research." *Sociological Methodology* 25: 111. https://doi.org/10.2307/271063.

Richie-Halford, A., M. Cieslak, L. Ai, et al. 2022. "An Analysis-Ready and Quality Controlled Resource for Pediatric Brain White-Matter Research." *Scientific Data* 9, no. 1: 616. https://doi.org/10.1038/s41597-022-01695-7.

Roddy, D. W., E. Roman, A. Nasa, et al. 2022. "Microstructural Changes Along the Cingulum in Young Adolescents With Psychotic Experiences: An Along-Tract Analysis." *European Journal of Neuroscience* 56, no. 7: 5116–5131. https://doi.org/10.1111/ejn.15806.

Sagarwala, R., and H. A. Nasrallah. 2021. "The Effect of Antipsychotic Medications on White Matter Integrity in First-Episode Drug-naïve Patients With Psychosis: A Review of DTI Studies." *Asian Journal of Psychiatry* 61: 102688. https://doi.org/10.1016/j.ajp.2021.102688.

Schoorl, J., M. C. Barbu, X. Shen, et al. 2021. "Grey and White Matter Associations of Psychotic-Like Experiences in a General Population Sample (UK Biobank)." *Translational Psychiatry* 11, no. 1: 21. https://doi.org/10.1038/s41398-020-01131-7.

Schumann, G., E. Loth, T. Banaschewski, et al. 2010. "The IMAGEN Study: Reinforcement-Related Behaviour in Normal Brain Function and Psychopathology." *Molecular Psychiatry* 15, no. 12: 1128–1139. https://doi.org/10.1038/mp.2010.4.

Smigielski, L., P. Stämpfli, D. Wotruba, et al. 2022. "White Matter Microstructure and the Clinical Risk for Psychosis: A Diffusion Tensor Imaging Study of Individuals With Basic Symptoms and at Ultra-High Risk." *NeuroImage: Clinical* 35: 103067. https://doi.org/10.1016/j.nicl.2022.103067.

Smith, R., D. Christiaens, B. Jeurissen, et al. 2021. "On false positive control in Fixel-Based Analysis. International Society for Magnetic Resonance in Medicine." https://www.researchgate.net/publication/351736236_On_false_positive_control_in_Fixel-Based_Analysis.

Smith, R., T. Dhollander, and A. Connelly. 2019. "On the Regression of Intracranial Volume in Fixel-Based Analysis." https://www.researchgate.net/publication/332857716_On_the_regression_of_intracranial_volume_in_Fixel-Based_Analysis.

Smith, R., J.-D. Tournier, F. Calamante, and A. Connelly. 2013. "SIFT: Spherical-Deconvolution Informed Filtering of Tractograms." *NeuroImage* 67: 298–312. https://doi.org/10.1016/j.neuroimage.2012.11.049.

Stämpfli, P., S. Sommer, A. Manoliu, et al. 2019. "Subtle White Matter Alterations in Schizophrenia Identified With a New Measure of Fiber Density." *Scientific Reports* 9, no. 1: 1. https://doi.org/10.1038/s41598-019-40070-2.

Szeszko, P. R., D. G. Robinson, T. Ikuta, et al. 2014. "White Matter Changes Associated With Antipsychotic Treatment in First-Episode Psychosis." *Neuropsychopharmacology* 39, no. 6: 1324–1331. https://doi.org/10.1038/npp.2013.288.

Tournier, J.-D., F. Calamante, and A. Connelly. 2010. "Improved Probabilistic Streamlines Tractography by 2nd Order Integration Over Fibre Orientation Distributions." *International Society for Magnetic Resonance in Medicine*. https://cds.ismrm.org/protected/10MProceedings/PDFfiles/1670_4298.PDF.

Tournier, J.-D., S. Mori, and A. Leemans. 2011. "Diffusion Tensor Imaging and Beyond." *Magnetic Resonance in Medicine* 65, no. 6: 1532–1556. https://doi.org/10.1002/mrm.22924.

Tournier, J.-D., R. Smith, D. Raffelt, et al. 2019. "MRtrix3: A Fast, Flexible and Open Software Framework for Medical Image Processing and Visualisation." *NeuroImage* 202: 116137. https://doi.org/10.1016/j.neuroimage.2019.116137.

van Os, J., and U. Reininghaus. 2016. "Psychosis as a Transdiagnostic and Extended Phenotype in the General Population." *World Psychiatry: Official Journal of the World Psychiatric Association (WPA)* 15, no. 2: 118–124. https://doi.org/10.1002/wps.20310.

Veraart, J., E. Fieremans, and D. S. Novikov. 2016. "Diffusion MRI Noise Mapping Using Random Matrix Theory." *Magnetic Resonance in Medicine* 76, no. 5: 1582–1593. https://doi.org/10.1002/mrm.26059.

Wagenmakers, E.-J., M. Marsman, T. Jamil, et al. 2018. "Bayesian Inference for Psychology. Part I: Theoretical Advantages and Practical Ramifications." *Psychonomic Bulletin & Review* 25, no. 1: 35–57. https://doi.org/10.3758/s13423-017-1343-3.

Wasserthal, J., P. Neher, and K. H. Maier-Hein. 2018. "TractSeg—Fast and Accurate White Matter Tract Segmentation." *NeuroImage* 183: 239–253. https://doi.org/10.1016/j.neuroimage.2018.07.070.

Waszczuk, K., K. Rek-Owodziń, E. Tyburski, M. Mak, B. Misiak, and J. Samochowiec. 2021. "Disturbances in White Matter Integrity in the Ultra-High-Risk Psychosis State—A Systematic Review." *Journal of Clinical Medicine* 10, no. 11: 11. https://doi.org/10.3390/jcm10112515.

Yao, L., S. Lui, Y. Liao, et al. 2013. "White Matter Deficits in First Episode Schizophrenia: An Activation Likelihood Estimation Meta-Analysis." *Progress in Neuro-Psychopharmacology and Biological Psychiatry* 45: 100–106. https://doi.org/10.1016/j.pnpbp.2013.04.019.

Supporting Information

Additional supporting information can be found online in the Supporting Information section. **Table S1:** Participant characteristics across each scanning site in Study 2 ($n = 1098$) in mean (sd). **Figure S1:** Whole-brain average FDC values plotted against standardised psychotic-like experiences scores in (A) Study 1 ($n = 41$) and (B) Study 2 ($n = 1098$). **Table S2:** Number of fixels in each tract as extracted from tractseg across Study 1 and Study 2.